Polyetherimide/Bucky Gels Nanocomposites with Superior Conductivity and Thermal Stability

Ye Chen,[†] Jing Tao,[†] Lin Deng,[†] Liang Li,[‡] Jun Li,[‡] Yang Yang,[‡] and Niveen M. Khashab*,[†]

[†]Controlled Release and Delivery Lab, Advanced Membranes and Porous Materials Center, King Abdullah University of Science and Technology (KAUST), Thuwal 23955-6900, Kingdom of Saudi Arabia

[‡]Advanced Nanofabrication, Imaging and Characterization Core lab, King Abdullah University of Science and Technology (KAUST), Thuwal 23955-6900, Kingdom of Saudi Arabia

S *Supporting Information*

ABSTRACT: Polyetherimide (PEI) nanocomposites comprising bucky gels of industrial-grade multiwalled carbon nanotubes (MWCNTs) and ionic liquid (IL, 1-butyl-3-methyl imidazolium hexafluorophosphate ([BMIM][PF$_6$])) were prepared. The processing framework for this nanocomposite is simple, reproducible, and easily scalable. The strong interaction between IL and MWCNTs caused the latter to uniformly disperse in the PEI matrix while IL flowed into the gaps between the nanotubes' walls. The nanocomposite exhibited an enhanced conductivity of 2.01 × 10^4 Ω·cm volume resistivity at room temperature; the value decreased dramatically by 12 orders of magnitude, compared to pristine PEI. The IL free ions and MWCNTs networks provided excellent channels for electron transfer. PEI/bucky gels nanocomposites also showed improved thermal stability and high tensile strength. Other than having antiwear properties, this material can have numerous applications in the aerospace and electronics industries. Moreover, our work presents a "green" method toward modified nanocomposites industrial production as IL is environmentally safe and is easily recyclable.

KEYWORDS: PEI, MWCNT, nanocomposites, ionic liquid, mechanical properties, conductivity
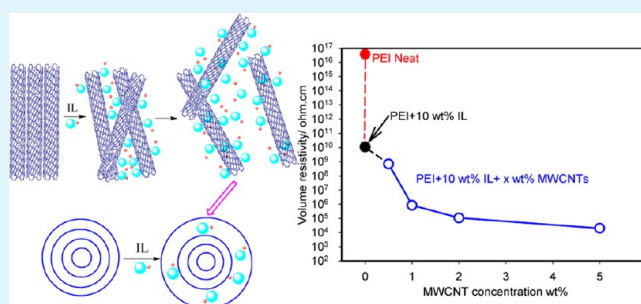
INTRODUCTION

Polymer/carbon nanotubes (CNTs) composites are engineered to have the good processability characteristics of the polymer and the excellent functional properties of CNTs. The critical challenge remains in enhancing the dispersion and alignment of CNTs in the polymer matrix.[1] In recent years, there have been many efforts to improve the dispersion of CNTs in polymer composites. These include studies on covalent[2−8] and noncovalent[9−15] bonding between CNTs and polymers. While covalent bonding methods introduce defects to the CNTs, noncovalent bonding methods require complex and lengthy pretreatment techniques. Thus, designing a simple and reproducible method for functionalized CNTs to be uniformly incorporated in polymer matrices is an important objective in order to scale-up the production and eventually commercial use of CNT nanocomposites.

Room temperature imidazolium-based ionic liquids (ILs) were used to disperse single walled carbon nanotubes (SWCNTs) to form what was called "bucky gel".[16] Ionic liquids (ILs) are usually composed of large organic cations and either inorganic or organic anions. When used as solvents, ILs have many advantages,[17] such as extremely low volatility and toxicity, excellent thermal and chemical stability, high ionic conductivity, and ease of recycling. ILs are considered to be "green solvents" and promising replacements for traditional

organic solvents.[18,19] IL molecules were found to interact with the π-electronic surfaces of the SWCNTs by means of cation-π/π−π interactions, which disperse the SWCNTs.[20,21] The interaction of ILs with carbon nanotubes was further studied using Raman and IR spectroscopy where it was discovered that ILs interacted with carbon nanotubes through weak van der Waals interactions rather than just "cation-π" interactions.[22,23] Tour et al. found that ILs can be used for green chemical functionalization of carbon nanotubes by grinding them for several minutes at room temperature to obtain individualized nanotube structures.[24] The use of ILs suggested the possibility of processing CNT−IL "bucky gels" on a large scale using mechanical grinding.[25−27] Applications using CNTs dispersed in ILs have been reported in sensors, actuators, and electrochemistry.[28−34]

Combining the properties of ILs and CNTs can provide many advantages in polymer processing. On one hand, ILs can be used as plasticizers or lubricants for polymers with high melting temperature, high glass transition temperature, or poor fluidity in melting.[34,35] On the other hand, CNTs can be dispersed well in ILs, suggesting a simple and feasible method
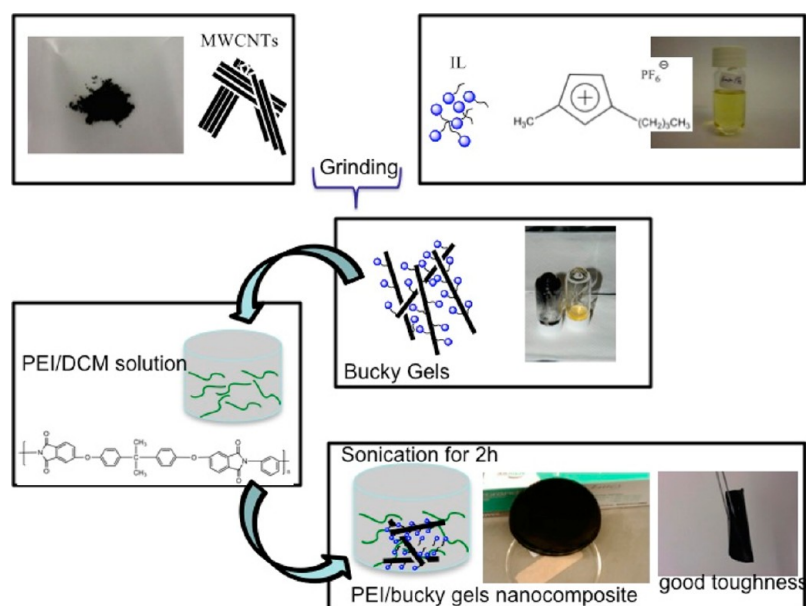
Figure 1. Processing of PEI/bucky gels nanocomposites. The obtained composites had good toughness as the film could be curved adequately without any damage.

to make high-performance nanocomposites with CNTs. Few reports were published on the polymerization of IL monomers with CNTs to form IL−polymer films; however, the cost of ionic liquid polymers is high, and they are not commercially produced by plastics companies.[36−40] Thus, an easy and fast processing method to prepare plastic composites based on multiwalled carbon nanotubes (MWCNTs)−IL gels remains illusive.

Toward this goal, bucky gels with MWCNTs and a common short chain IL, 1-butyl-3-methyl imidazolium hexafluorophosphate ([BMIM][PF$_6$]), were prepared and uniformly incorporated in polyetherimide (PEI) matrix to make high performance thermoplastic nanocomposite. Compared with long chain ILs, short chain ILs are liquid at room temperature, making it easier for IL molecules to interact with CNTs upon grinding. The strong interaction of IL with MWCNTs, the existence of free IL ions in polymer matrix, and the interfacial interaction between all components (MWCNTs, IL, and polymer chains) afforded highly conductive and thermally stable nanocomposites. The tested nanocomposite samples were prepared via a straightforward solution casting method that is both simple and scalable.

EXPERIMENTAL SECTION

Materials. Polyetherimide (PEI) chips supplied by SABIC Innovative Plastics under the trade name of grade ULTEM 1000P were used as received. MWCNTs were purchased from Nanolab Inc. with diameters of 10−30 nm, lengths of 5−20 μm, and purity of 90% (industrial grade). 1-Butyl-3-methyl imidazolium hexafluorophosphate ([BMIM][PF$_6$], 97%) was purchased from Sigma-Aldrich and was vacuum-dried at 60 °C for 24 h to remove any moisture before use. Structures of material used are provided in Figure 1.

Processing of PEI/Bucky Gels Nanocomposites. To prepare MWCNTs/[BMIM][PF$_6$] gel (1/4 ratio), pristine MWCNTs (10 mg) were first mixed with [BMIM][PF$_6$] (40 mg) and then grinded for 30 min. MWCNTs were able to disperse uniformly into [BMIM][PF$_6$] to afford a sticky black gel. Ionic liquids potentially have a high affinity toward MWCNTs structure due to "cation-π" interactions and/or van der Waals interaction.[26] The gels were made in different ratios by weight of MWCNTs to [BMIM][PF$_6$] from 1:4 to 1:200. Each gel was then added into a PEI/DCM solution, stirred

overnight followed by sonication for 2 h. A black homogeneous solution was then obtained and casted into a composite membrane at room temperature for further characterization. The amount of IL used was 2 wt %, 5 wt %, 10 wt %, 20 wt %, 30 wt %, 40 wt %, and 50 wt % of the composites, and the amount of MWCNTs used was 0.1 wt %, 0.5 wt %, 1 wt %, 2 wt %, and 5 wt % of the composites. The overall process of preparing MWCNT−IL gels and PEI/bucky gels composite films is presented in Figure 1. The composites had good toughness as the film could be curved adequately without any damage (Figure 1).

INSTRUMENTATION

Raman spectroscopy was performed with an ARAMIS UV (HORIBA) Raman Microscope, which was equipped with a 100mW diode laser with an excitation wavelength of 785 nm. The X-ray powder diffraction (XRD) patterns were obtained from MWCNT and IL mixtures by a Bruker D8 Advance (40 KV, 40 mA) with Cu Kα (λ = 1.5406 Å) irradiation at a scanning rate of 2°/min in the 2θ range of 10−50°. The morphological study of the composite was conducted on a FEI Magellan/Quanta600 FEGSEM (USA) electron scanning electron microscope (SEM). The cryo-fractured surfaces were coated with a thin layer of gold (5 nm). The vacuum was on the order of 10^{-4}−10^{-6} mmHg during scanning of the composite samples.

Dynamic mechanical thermal analysis (DMA) was performed on DMA 242C (Netzsch, Germany) in the thin tension mode, at a constant frequency of 1 Hz, with the static force at 0.3 N, the dynamic force at 0.2 N, a heating rate of 2 K/min under a nitrogen atmosphere, and in the temperature range of 50 to 230 °C. Tensile testing was done on a commercial universal testing machine (Changchun Zhineng Company, China) at room temperature with a crosshead speed of 5 mm/min. Specimens were cut from the casted films with 50 mm gauge lengths and 10 mm widths. The decomposition behavior of the composites was studied using thermogravimetric analysis (TGA) on a TG 209 F1 Iris (Netzsch, Germany) thermogravimetric analyzer in a nitrogen atmosphere from 30 to 600 °C, with a heating rate of 10 °C/min. The thermal behavior of the nanocomposites was studied using a differential scanning calorimeter (DSC 204 F1
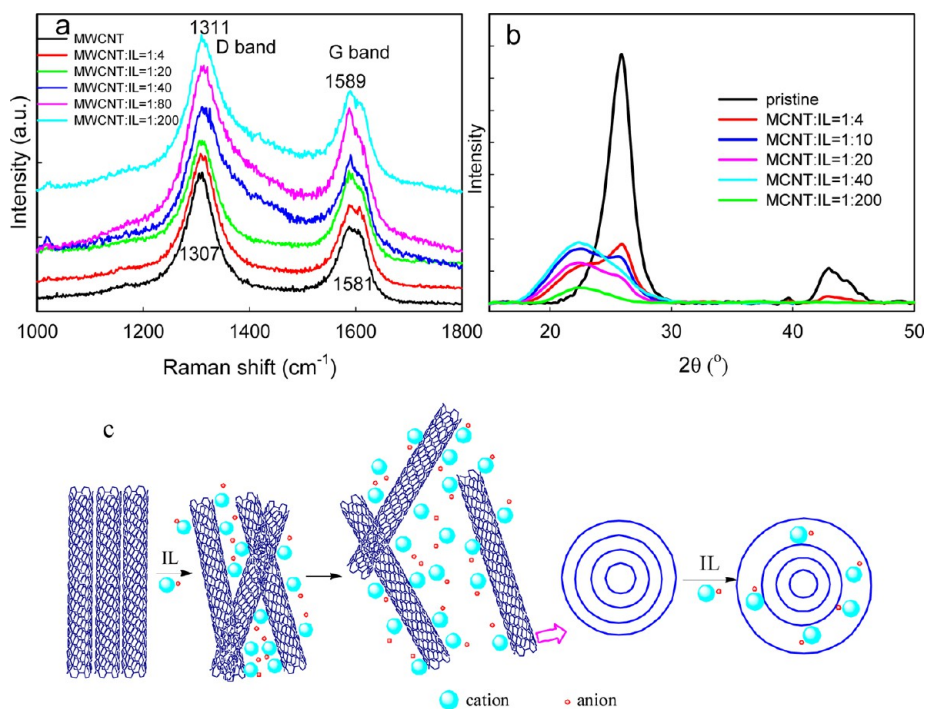
Figure 2. (a) Raman spectra and (b) XRD spectra of pristine and modified MWCNTs. (c) Proposed schematic of the interaction between ionic liquid and MWCNTs.

Phoenix, Netzsch, Germany). The heating rate was 10 °C/min under a nitrogen atmosphere with a flow rate of 40 mL/min.

The electrical conductivities of the samples were measured as follows: specimens were cut from the edge of each PEI nanocomposite film toward the center with 30 mm lengths, 10 mm widths, and 0.3−0.5 mm thickness. A constant voltage of 100 V DC was applied across the specimen using a Keithley model 248 high voltage supply (USA), and the current was monitored with a Keithley 6517B (USA) electrometer. The results were obtained by averaging the conductivities from three different specimens for each nanocomposite film.

■ RESULTS AND DISCUSSION

Bucky gels were prepared by grinding MWCNTs with [BMIM][PF$_6$] for 30 min until a black gel was obtained. Raman spectroscopy and X-ray diffraction (XRD) were utilized to characterize the obtained gels. Raman spectra of the pristine MWCNT and bucky gels are shown in Figure 2a. The peak at 1580 cm^{-1} corresponds to the G band, which is used as a fingerprint to identify the existence of ordered hexagonal structures in carbon-related materials, such as carbon nanotubes, graphite, and graphene.[41−44] The peak at 1300 cm^{-1} corresponds to the D band (disorder-induced mode)[45] which originates from various disorders, such as confined shapes, edges, doping, and atomic defects.[46] The relative intensity between the D and the G bands is known to be a good indicator of the quantity of structural defects. For pristine MWCNTs, the D band is higher than the G band, indicating there are many defects in our as-received MWCNTs. Interaction of IL with MWCNTs was evident in the slight Raman shift of the MWCNT/gels when the concentration of the IL was increased. Compared with pristine MWCNT, there was a 4 cm^{-1} upshift of the D band and an 8 cm^{-1} upshift of the G band in the MWCNT−IL = 1:200 gel, and no new vibrations were observed. The upshift is due to adhesion of the IL

molecules via cation-π/π−π interactions onto the nanotube surfaces and/or perturbation of π−π stacking of the multiwalls of the nanotubes.

We further confirmed the interaction of IL with MWCNTs by XRD. As shown in Figure 2b, there is an obvious narrow peak observed at $2\theta = 25.9°$ ($d = 0.34$ nm) in pristine MWCNT, which indicates the interplanar spacing of tube walls in individual MWCNTs. When the concentration of the IL in the bucky gel was increased, this peak became smoother and broader, indicating an interaction between the IL molecules and the MWCNTs. As shown in the curves for the MWCNT−IL = 1:4, 1:10, and 1:20 gels, two peaks divided away from the narrow peak, with the larger peak becoming smoother and the smaller peak becoming more obvious as the concentration of IL increased. The smaller diffraction peak may be from the liquid crystalline phase of IL, which can be observed in ILs with the number of carbons in the alkyl chains greater than 12,[47] or in the solid phase of the IL.[48] For [BMIM][PF$_6$], this diffraction pattern is difficult to observe (we found that pure [BMIM]-[PF$_6$] had no diffraction peak, data not shown) because it is liquid at room temperature and has short-chain cations. When the concentration ratio was 1:40 or 1:200, there was almost only one broad peak observed. The disappearance of another larger peak at 42.9° ($d = 0.21$ nm) with increasing IL concentration further confirmed the interaction between IL molecules and MWCNTs. The suggested interaction schematic of IL with MWCNTs is shown in Figure 2c. It is evident from the obtained data that the distance between individual MWCNTs enlarges with increasing IL concentration. Meanwhile, the IL molecules flowed into the gaps between the walls of the nanotubes interacting with the inside surfaces of the walls as well as the outside surfaces, leading to an expansion of gaps between the walls in an individual MWCNT. The existence of ILs in the gaps between the tube walls improves the electrical
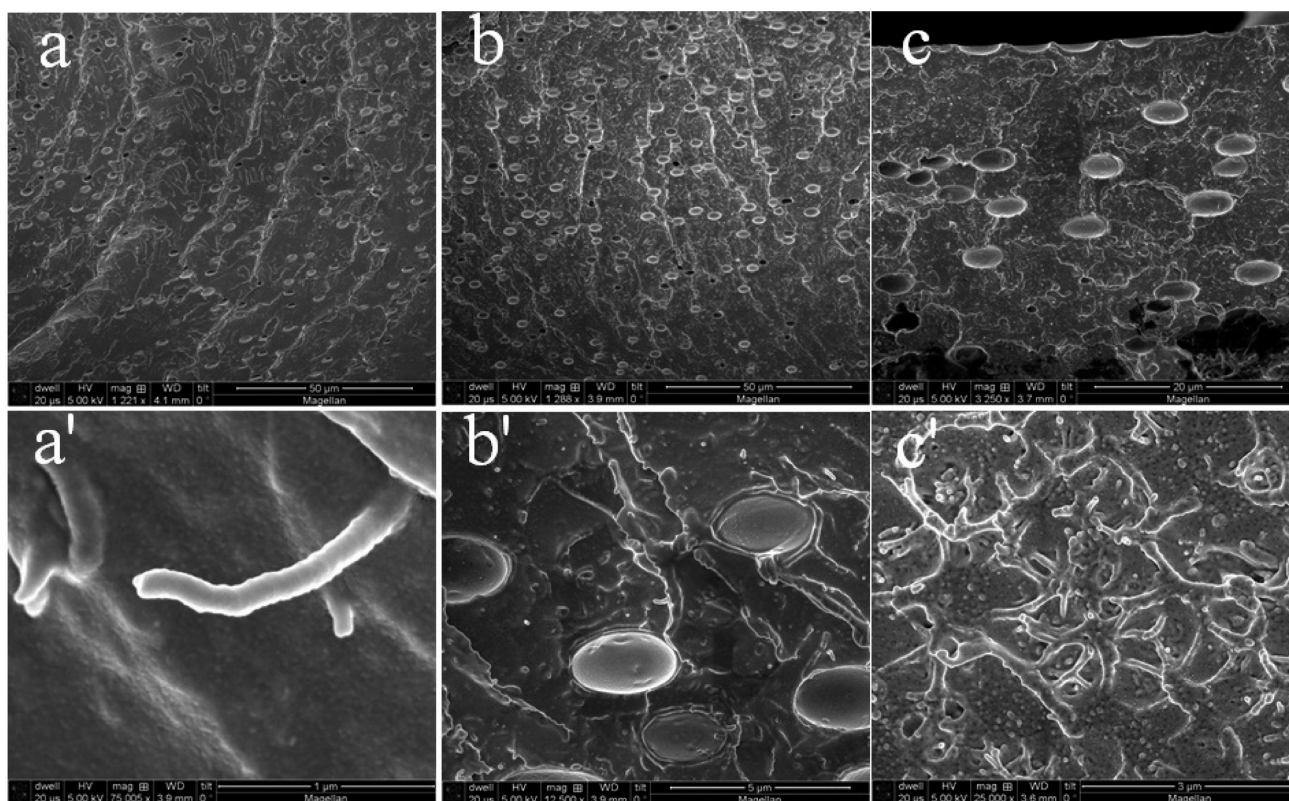
Figure 3. SEM images of PEI composite films with 10 wt % IL and different MWCNT concentrations. (a) 0.5 wt % MWCNTs; (b) 2.0 wt % MWCNTs; (c) 5.0 wt % MWCNTs; (a′), (b′), and (c′) show magnified images of (a), (b), and (c), respectively.
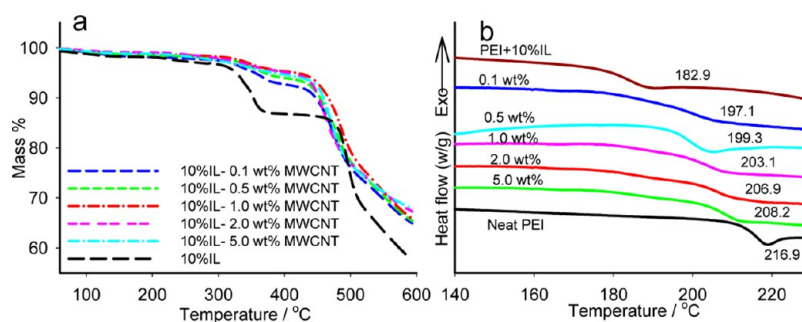

Figure 4. (a) TGA and (b) a glass transition temperature plot of PEI-10 wt % IL and its MWCNT composites.

properties of MWCNTs and as a result promotes electron transfer in the composite.

Bucky gels were then added into a PEI/DCM solution which was stirred and sonicated before casting into a composite membrane. SEM images (Figure 3) of the cryo-fractured surfaces of PEI/IL−MWCNT composites show that MWCNTs are homogeneously dispersed at the individual level throughout the PEI matrix, with no obvious MWCNTs aggregation. The diameter of MWCNT (100−200 nm) is much wider compared to pristine MWCNTs (10−30 nm) suggesting that MWCNTs are wrapped by the polymer chains (Figure 3a′). Figure 3c shows the SEM of the PEI composite with 10% IL and 5.0 wt % MWCNTs concentrations. There is an abundance of fine and well-dispersed MWCNTs almost throughout the PEI matrix, together with a slight agglomerate in a part of the matrix. The interaction of IL with MWCNT helps to prevent nanotube aggregation and results in a controlled morphology. In addition, a network of MWCNTs can be observed on the surface as MWCNTs overlap in the PEI

matrix and are linked by MWCNT bridges (Figure 3c′). Other researchers have observed similar network morphologies.[49,50] This network is very important for improving the conductivity of PEI composites as it promotes electron transfer throughout the polymer matrix.

The thermal behaviors of PEI/IL composite membranes with different MWCNT concentration were studied by TGA analysis. Two steps were observed in the thermal degradation of all samples under an N_2 atmosphere, as shown in Figure 4a. The first peak corresponds to the decomposition of IL itself. The main decomposition step of PEI was increased with increasing MWCNT concentration, and it reached a maximum value at 1.0 wt %. The data is summarized in Table 1.

Increasing the concentration of modified MWCNTs added to the composite slows the composites' volatilization and/or decomposition rates down. As a strong interfacial interaction exists between MWCNTs and the polymer (SEM images), we hypothesize that polymer chains wrapping the well-dispersed MWCNTs have a restricted activity, which induced the thermal
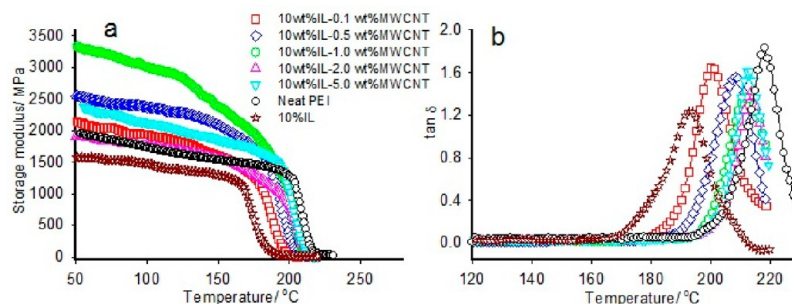
Table 1. Thermal Properties of PEI-10 wt % IL Composite and Its Composites with Different MWCNTs Concentration

MWCNT wt %	temp. at 5 wt % weight loss (°C)	temp. at 10 wt % weight loss (°C)	T_g by DSC (°C)	T_g by DMA (°C)
0	328	353	182.9	190.2
0.1	354	445	197.1	199.9
0.5	368	453	199.3	208.1
1.0	413	468	203.1	212.2
2.0	408	450	206.9	213.2
5.0	383	459	208.2	213.5

Table 2. Mechanical Properties of Neat PEI and Its Composites

		storage modulus at 100 °C (GPa)	tensile strength (MPa)	tensile modulus (GPa)	elongation at break (%)
neat PEI		1.73	78.6	1.67	22
PEI/10 wt % IL		1.48	63.1	1.56	9.7
MWCNT wt %	0.1	1.94	81.0	1.82	5.9
	0.5	2.37	87.2	2.08	5.0
	1.0	3.01	110.8	2.21	6.8
	2.0	1.76	73.2	1.92	4.3
	5.0	2.12	90.5	2.06	7.7

resistance of the matrix.[50] By increasing the amount of well dispersed MWCNTs, the amount of restricted segment in the polymer matrix increased and subsequently led to an increase in the decomposition temperature of the polymer. On the other hand, aggregation of MWCNT (2.0 wt %, Figure 3b′) may restrict polymer chain wrapping and thus result in a mild reduction in the decomposition temperature.

DSC curves indicate the distinct glass transition temperature (T_g) of the PEI/bucky gel composite (with different contents of MWCNTs). IL is a good plasticizer for PEI as a small amount of IL reduces the glass transition temperature of PEI (Table 1). Compared to neat PEI, T_g decreased by about 34 °C after addition of 10 wt % IL (from 216.9 to 182.9 °C). However, T_g is increased by adding MWCNTs. The T_g of the composite increased by about 14 °C after incorporating 0.1 wt % MWCNTs into the PEI/IL composite (from 182.9 to 197.1 °C), which supports that the mobility of the polymer chains is reduced due to the constraining effect of MWCNTs. In short, IL decreases the glass transition temperature of the composite, while well-dispersed MWCNTs increase it.

Figure 5 shows the DMA curves as a function of temperature for PEI and its nanocomposites. Compared with neat PEI, the storage modulus ($E′$) of the PEI composites with 10 wt % IL is lower than the storage modulus for PEI/bucky gel composites (Figure 5a). The storage modulus is increased significantly with increasing MWCNT concentration from 0 to 1.0 wt %. At a concentration of 2.0 wt %, it decreased, but it increased again at 5.0 wt % MWCNTs. The results are summarized in Table 2. We ascribe the significant improvement in the storage modulus of PEI nanocomposites to the combined effect of high strength and the fine dispersion of MWCNTs filler. Though the storage modules decreased with the addition of IL, it was improved by adding MWCNT to the composite. The reduction in the storage modulus at 2.0 wt % MWCNTs was caused by the slight aggregation of MWCNTs, while the increase again at the 5.0 wt % MWCNTs was caused by the vast formation of the

MWCNTs networks in PEI matrix which requires greater external force to break down.

The tensile properties of the composites with 10 wt % IL decreased, compared with the tensile strength of neat PEI (Figure 6). The tensile strength and tensile modulus decreased
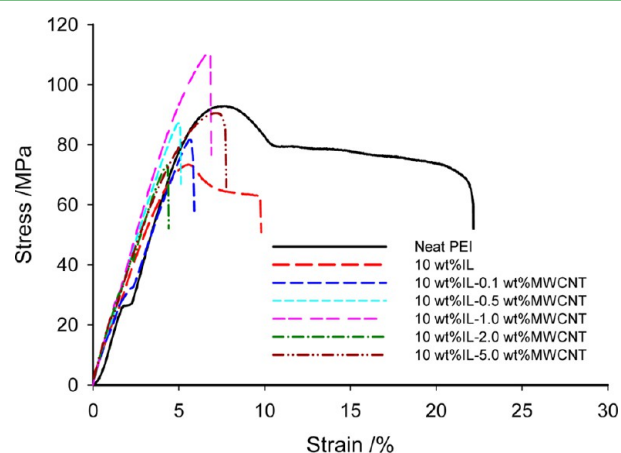
Figure 6. Typical stress−strain curves for neat PEI and its composites with 10 wt % IL and different MWCNT concentration.

from 78.6 to 63.1 MPa and from 1.67 to 1.56 GPa, respectively. However, with the addition of a small amount of MWCNTs, the tensile properties of composites improved and surpassed those of neat PEI. We determined that the PEI/bucky gel composite with 1.0 wt % MWCNTs loading was the best. The tensile strength of PEI improved by about 76% from 63.1 to 110.8 MPa, and the tensile modulus improved by about 42% from 1.56 to 2.21 GPa. A pronounced yield and postyield drop were observed for neat PEI and PEI/IL composites while there

Figure 5. DMA results for PEI and its composites with 10 wt % IL and different MWCNT concentrations. (a) storage modulus curves; (b) loss factor tan δ versus temperature.

7482

dx.doi.org/10.1021/am401792c | ACS Appl. Mater. Interfaces 2013, 5, 7478−7484

was no pronounced yield for MWCNT−reinforced PEI nanocomposites. Therefore, by adding a small amount of functionalized MWCNTs, the nanocomposite films become stiffer and stronger due to the strong interfacial interactions between the nanotubes and the PEI matrix. Furthermore, the best elongation at break of the PEI/bucky gel composite was observed at 5.0 wt % MWCNTs loading, due to the formation of MWCNTs networks in the polymer matrix. In addition, the tensile properties of PEI/bucky gel composites with 1.0 wt % MWCNTs and different IL content are also reported (Figure S1, Supporting Information). Compared with neat PEI, tensile strength changes are minor with only 1.0 wt % MWCNT (without IL) but improved a lot with 10 wt % IL and 1.0 wt % MWCNTs. The reason is that MWCNTs modified with IL have a better dispersion profile in PEI matrix compared to MWCNTs without modification. However, by increasing IL content in composites, the tensile strength is decreased and the elongation at break is increased which indicates that the composites become weaker but more flexible. Moreover, PEI/IL samples with no MWCNTs showed the lowest thermal stability as well as the weakest mechanical profile. Thus, although using IL boosts conductivity, CNTs are crucial to maintain thermal and mechanical integrity of the polymer matrix (Figures S2−S4, Supporting Information).

It is well accepted that IL can provide free ions for electron transfer and that carbon nanotubes are among the best nanofillers to improve the conductivity of materials.[31,51] Bucky gels combine both the advantages of ILs and carbon nanotubes so the conductivity of our different composite samples was tested and compared. The room temperature volume resistivity of PEI and PEI/bucky gel composites with 10 wt % IL and various concentrations of MWCNT are shown in Figure 7. The addition of 10 wt % IL loading was chosen in our
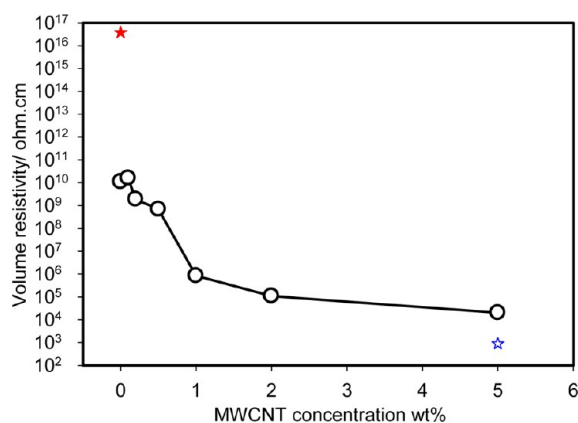

Figure 7. The volume resistivity of PEI composites with 10 wt % IL and different MWCNTs concentrations at room temperature. The red solid star indicates the resistivity of neat PEI; the blue hollow star indicates the resistivity of the PEI composite with 50 wt % IL and 5.0 wt % MWCNTs.

experiment, because we determined that it was the breaking point for the increasing conductivity of PEI (see Supporting Information). The electrical resistivity decreased (conductivity increased) generally as the content of MWCNTs increased. It decreased significantly when the MWCNTs content is at 1.0 wt % (from 9.89×10^9 to 8.39×10^5 Ω·cm). This value slightly decreased with increasing MWCNTs content to about 2.01×10^4 Ω·cm at loading of 5.0 wt % MWCNTs. Compared with

pristine PEI (3.82×10^{16} Ω·cm, red solid star in Figure 7), the volume resistivity of composites with 10 wt % IL and 5 wt % MWCNTs decreased dramatically by 12 orders of magnitude. Furthermore, the resistivity decreased by about 14 orders of magnitude with 5.0 wt % loading of MWCNTs and 50 wt % IL. At this point, the composite can be considered to be a good semiconductor, compared with neat PEI.

To our best knowledge, our obtained resistivity value is the lowest for PEI composites (with the same pristine MWCNT loading) to be reported. Isayev et al.[52] used an ultrasonically assisted twin screw extrusion to mix PEI and MWCNTs. The obtained composites had a sharp decrease on volume resistivity at 2.0 wt % of MWCNTs loading. The lowest value achieved at 5.0 wt % MWCNTs was 10^6 Ω·cm. Kumar et al.[50] found that the conductivity of PEI could be improved by using MWCNT via a facile solution processing method, and the volume resistivity could be decreased to 10^5 Ω·cm after loading 5.0 wt % MWCNT. This improvement is likely due to the continuous IL phase, which provides an extensive area for electron transfer. Moreover, the formation of MWCNTs networks provides more channels for electrons to transfer throughout the matrix (Figure 3c′). IL molecules trapped in the gaps of the tube walls may also have a role in enhancing electron migration through each tube's walls and consequently through the whole matrix (Figure 2c).

CONCLUSION

A simple and scalable processing method of high performance PEI/bucky gel nanocomposites is described. Bucky gels were mixed with PEI solution to obtain a nanocomposite film with high conductivity and thermal stability by a simple solution casting method. The most interesting aspects of this nano-composite processing are that it uses relatively low cost industrially produced IL and MWCNTs and that by varying IL to MWCNT ratio multipurpose composites can be easily produced (electrical and mechanical profiles can be easily tailored). We are currently expanding this method to other thermoplastics such as polycarbonate (PC) and poly(methyl methacrylate) (PMMA).

ASSOCIATED CONTENT

S **Supporting Information**

Typical stress−strain curves of PEI composite with 1.0 wt % of MWCNTs and different ionic liquid (IL) concentrations. SEM images, TGA, and DSC curves of PEI composites with different IL concentrations. This information is available free of charge via the Internet at http://pubs.acs.org/.

AUTHOR INFORMATION

Corresponding Author

*Tel:+96628021172. Fax:+96628082410. E-mail: niveen.khashab@kaust.edu.sa.

Notes

The authors declare no competing financial interest.

ACKNOWLEDGMENTS

■ REFERENCES

(1) Chakraborty, A. K.; Coleman, K. S. *J. Nanosci. Nanotechnol.* **2008**, *8*, 4013−4016.

(2) Karousis, N.; Tagmatarchis, N.; Tasis, D. *Chem. Rev.* **2010**, *110*, 5366−5397.

(3) Price, B. K.; Tour, J. M. *J. Am. Chem. Soc.* **2006**, *128*, 12899−12904.

(4) Hu, H.; Zhao, B.; Hamon, M. A.; Kamaras, K.; Itkis, M. E.; Haddon, R. C. *J. Am. Chem. Soc.* **2003**, *125*, 14893−14900.

(5) Coleman, K. S.; Bailey, S. R.; Fogden, S.; Green, M. L. H. *J. Am. Chem. Soc.* **2003**, *125*, 8722−8723.

(6) Ge, J. J.; Zhang, D.; Li, Q.; Hou, H. Q.; Graham, M. J.; Dai, L. M.; Harris, F. W.; Cheng, S. Z. D. *J. Am. Chem. Soc.* **2005**, *127*, 9984−9985.

(7) Blake, R.; Coleman, J. N.; Byrne, M. T.; McCarthy, J. E.; Perova, T. S.; Blau, W. J.; Fonseca, A.; Nagy, J. B.; Gun'ko, Y. K. *J. Mater. Chem.* **2006**, *16*, 4206−4213.

(8) Yu, B.; Zhou, F.; Liu, G.; Liang, Y.; Huck, W. T. S.; Liu, W. M. *Chem. Commun.* **2006**, 2356−2358.

(9) Krstic, V.; Duesberg, G. S.; Muster, J.; Burghard, M.; Roth, S. *Chem. Mater.* **1998**, *10*, 2338−2340.

(10) Star, A.; Stoddart, J. F.; Steuerman, D.; Diehl, M.; Boukai, A.; Wong, E. W.; Yang, X.; Chung, S. W.; Choi, H.; Heath, J. R. *Angew. Chem., Int. Ed.* **2001**, *40*, 1721−1725.

(11) Coleman, J.; Dalton, A.; Curran, S.; Rubio, A.; Davey, A.; Drury, A.; McCarthy, B.; Lahr, B.; Ajayan, P.; Roth, S.; Barklie, R.; Blau, W. *Adv. Mater.* **2000**, *12*, 401−401.

(12) Li, L. Y.; Li, C. Y.; Ni, C. Y. *J. Am. Chem. Soc.* **2006**, *128*, 1692−1699.

(13) Suri, A.; Chakraborty, A. K.; Coleman, K. S. *Chem. Mater.* **2008**, *20*, 1705−1709.

(14) Zhang, L.; Tao, T.; Li, C. Z. *Polymer* **2009**, *50*, 3835−3840.

(15) Vaisman, L.; Wagner, H. D.; Marom, G. *Adv. Colloid Interface Sci.* **2006**, *128*, 37−46.

(16) Fukushima, T.; Kosaka, A.; Ishimura, Y.; Yamamoto, T.; Takigawa, T.; Ishii, N.; Aida, T. *Science* **2003**, *300*, 2072−2074.

(17) Rebelo, L. P. N.; Lopes, J. N. C.; Esperanca, J.; Guedes, H. J. R.; Lachwa, J.; Najdanovic-Visak, V.; Visak, Z. P. *Acc. Chem. Res.* **2007**, *40*, 1114−1121.

(18) Earle, M. J.; Seddon, K. R. *Pure Appl. Chem.* **2000**, *72*, 1391−1398.

(19) Rogers, R. D.; Seddon, K. R. *Science* **2003**, *302*, 792−793.

(20) Fukushima, T.; Aida, T. *Chem.−Eur. J.* **2007**, *13*, 5048−5058.

(21) Bellayer, S.; Gilman, J. W.; Eidelman, N.; Bourbigot, S.; Flambard, X.; Fox, D. M.; De Long, H. C.; Trulove, P. C. *Adv. Funct. Mater.* **2005**, *15*, 910−916.

(22) Wang, J. Y.; Chu, H. B.; Li, Y. *ACS Nano* **2008**, *2*, 2540−2546.

(23) Wang, J. Y.; Li, Y. *J. Am. Chem. Soc.* **2009**, *131*, 5364−5365.

(24) Price, B. K.; Hudson, J. L.; Tour, J. M. *J. Am. Chem. Soc.* **2005**, *127*, 14867−14870.

(25) Sekitani, T.; Noguchi, Y.; Hata, K.; Fukushima, T.; Aida, T.; Someya, T. *Science* **2008**, *321*, 1468−1472.

(26) Lee, J.; Aida, T. *Chem. Commun.* **2011**, *47*, 6757−6762.

(27) Fukushima, T.; Aida, T. *Ionic liquids in polymer systems*; Brazel, C. S., Rogers, R. D., Eds.; Oxford University Press: New York, 2005; Vol. *913*, p 163−174.

(28) Likozar, B. *Soft Matter* **2011**, *7*, 970−977.

(29) Wei, D.; Baral, J. K.; Osterbacka, R.; Ivaska, A. *Nanotechnology* **2008**, *19*, 1−8.

(30) Subramaniam, K.; Das, A.; Heinrich, G. *Compos. Sci. Technol.* **2011**, *71*, 1441−1449.

(31) Terasawa, N.; Takeuchi, I.; Matsumoto, H.; Mukai, K.; Asaka, K. *Sens. Actuators, B: Chem.* **2011**, *156*, 539−545.

(32) Carrion, F. J.; Espejo, C.; Sanes, J.; Bermudez, M. D. *Compos. Sci. Technol.* **2010**, *70*, 2160−2167.

(33) Pauliukaite, R.; Murnaghan, K. D.; Doherty, A. P.; Brett, C. M. A. *J. Electroanal. Chem.* **2009**, *633*, 106−112.

(34) Carrion, F. J.; Sanes, J.; Bermudez, M. D.; Arribas, A. *Tribol. Lett.* **2011**, *41*, 199−207.

(35) Scott, M. P.; Brazel, C. S.; Benton, M. G.; Mays, J. W.; Holbrey, J. D.; Rogers, R. D. *Chem. Commun.* **2002**, 1370−1371.

(36) Marcilla, R.; Curri, M. L.; Cozzoli, P. D.; Martinez, M. T.; Loinaz, I.; Grande, H.; Pomposo, J. A.; Mecerreyes, D. *Small* **2006**, *2*, 507−512.

(37) Fukushima, T.; Kosaka, A.; Yamamoto, Y.; Aimiya, T.; Notazawa, S.; Takigawa, T.; Inabe, T.; Aida, T. *Small* **2006**, *2*, 554−560.

(38) Wu, B. H.; Hu, D.; Yu, Y. M.; Kuang, Y. J.; Zhang, X. H.; Chen, J. H. *Chem. Commun.* **2010**, *46*, 7954−7956.

(39) Liu, L.; Zheng, Z.; Gu, C. Y.; Wang, X. L. *Compos. Sci. Technol.* **2010**, *70*, 1697−1703.

(40) Chang, Y. H.; Lin, P. Y.; Wu, M. S.; Lin, K. F. *Polymer* **2012**, *53*, 2008−2014.

(41) Aljishi, R.; Dresselhaus, G. *Phys. Rev. B* **1982**, *26*, 4514−4522.

(42) Kawashima, Y.; Katagiri, G. *Phys. Rev. B* **1995**, *52*, 10053−10059.

(43) Dresselhaus, M. S.; Dresselhaus, G.; Saito, R.; Jorio, A. *Phys. Rep.* **2005**, *409*, 47−99.

(44) Malard, L. M.; Pimenta, M. A.; Dresselhaus, G.; Dresselhaus, M. S. *Phys. Rep.* **2009**, *473*, 51−87.

(45) Tuinstra, F.; Koenig, J. L. *J. Chem. Phys.* **1970**, *53*, 1126−1130.

(46) Wang, Y.; Alsmeyer, D. C.; Mccreery, R. L. *Chem. Mater.* **1990**, *2*, 557−563.

(47) Gordon, C. M.; Holbrey, J. D.; Kennedy, A. R.; Seddon, K. R. *J. Mater. Chem.* **1998**, *8*, 2627−2636.

(48) Consorti, C. S.; Suarez, P. A. Z.; de Souza, R. F.; Burrow, R. A.; Farrar, D. H.; Lough, A. J.; Loh, W.; da Silva, L. H. M.; Dupont, J. *J. Phys. Chem. B* **2005**, *109*, 4341−4349.

(49) Higgins, B. A.; Brittain, W. J. *Eur. Polym. J.* **2005**, *41*, 889−893.

(50) Kumar, S.; Li, B.; Caceres, S.; Maguire, R. G.; Zhong, W. H. *Nanotechnology* **2009**, *20*, 1−8.

(51) Baughman, R. H.; Zakhidov, A. A.; de Heer, W. A. *Science* **2002**, *297*, 787−792.

(52) Isayev, A. I.; Kumar, R.; Lewis, T. M. *Polymer* **2009**, *50*, 250−260.